

Corrosion Behavior of Gas Nitrided Bearing Steel

Venkatesh Begori¹, Anil Kumar Reddy Chinnagireddy^{2*}, Kasi Visheshwar Rao², Ashok Kumar Madupogu³, Venkat Ram Reddy Pandugula¹ and Sreekar Velineni⁵

¹Department of Mechanical Engineering, Vardhaman College of Engineering, Hyderabad, Telangana, India

²Department of Mechanical Engineering, KLEF, India

³Department of Mechanical Engineering, Narasimha Reddy Engineering College, Hyderabad, Telangana, India

*Correspondence to:

Anil Kumar Reddy Chinnagireddy
Department of Mechanical Engineering,
KLEF, India.

E-mail: anilreddymechnical@gmail.com

Received: September 15, 2023

Accepted: November 27, 2023

Published: November 30, 2023

Citation: Begori V, Chinnagireddy AKR, Rao KV, Madupogu AK, Pandugula VRR, et al. 2023. Corrosion Behavior of Gas Nitrided Bearing Steel. *NanoWorld J*9(S4): S361-S365.

Copyright: © 2023 Begori et al. This is an Open Access article distributed under the terms of the Creative Commons Attribution 4.0 International License (CCBY) (<http://creativecommons.org/licenses/by/4.0/>) which permits commercial use, including reproduction, adaptation, and distribution of the article provided the original author and source are credited.

Published by United Scientific Group

Abstract

Investigations have been made into the corrosion behavior of gas nitrided M50 bearing steel in corrosive media such as artificial sea water solution. Initially, the material is prepared by employing a tool like electrical discharge machining (EDM) cutting processes to create the precise needed dimensions of sample. Nano coatings play an important role in improving hardness, corrosion and wear resistance of metal, physical vapor deposition coating method by using TiC and N, was adopted for nano structured M50 martensite Steel. In this paper, to improve corrosion resistance, the material was gas nitrided. Using a variety of parameters, the electro potentiodynamic test is used to examine the corrosion resistance and surface roughness of these materials. With the aid of an electronic weighing balance, the necessary chemicals are added to create the seawater solution. The prepared solution is made available to the materials. Finally, the materials are taken away throughout various time frames. A potentiostat is used to measure the corrosion rates. Open circuit voltage (OCV) has been used to characterize corroded surfaces. For chosen samples with determined corrosive resistance, Tafel plots and open circuit potential (OCP) test graphs are created. The findings demonstrate that heat treatment improves the corrosion resistance of M50 steel.

Keywords

Corrosion behavior, M50, Sea water, Tafel plots, Gas nitride

Introduction

M50 is a special kind of steel created and manufactured to satisfy the exacting specifications of bearing applications. Bearings are essential parts utilized in a variety of machines and pieces of equipment to enable friction-free rotational movement. To acquire the desired hardness and toughness, bearing steels are subjected to specific heat treatment procedures, such as quenching and tempering [1]. With this heat treatment, the steel is guaranteed to have the necessary microstructure and mechanical characteristics to match the strict specifications of bearing applications [2]. The mechanical properties of a steel, which are typically ductility, hardness, yield strength, tensile strength, and impact resistance, are examined through heat treatment. In addition to creating hardness and softness, heat treatment also improves mechanical properties like tensile strength, yield strength, ductility, corrosion resistance, and creep rupture [3]. Additionally, these processes improve the machining's efficiency and adaptability. It is straightforward to alter the mechanical properties using heat treating to satisfy a particular design goal [4]. A premium melting alloy is M50. It offers exceptional resis-

tance to oxidation and great resistance to multiaxial stresses. Vacuum-induction melting, and vacuum-arc remelting techniques are used to refine the product. It has a high compressive strength that makes it ideal for a tool made of high-speed steel [5]. M50 steel is ideal for demanding bearing applications, especially in high-speed and aerospace applications, because of its exceptional high-temperature performance, wear resistance, and toughness. Obtaining the impact of heat treatment on bearing steel at various temperatures is the first goal of the current investigation [6]. Recognizing the phase transitions in heat-treated bearing steels and analyzing heat-treated bearing steels behave when exposed to seawater solution. The primary objective of the work is to investigate the behavior of the bearing steel before and after solutionizing and aging at various temperatures (using mechanical, corrosion, and OCP methods) [7]. Nanostructured coatings for M50 steel is used to modify surface properties like wear and corrosion resistance, where nitrogen is deposited on the surface of the component. Nanomaterials deposition will enhance major properties of material which can be done in physical and chemical deposition methods, where nano diamond coatings is sprayed on the metal surface in uniform way in presence of heat to cover the entire surface of specimen. Cost cutting and improvement of physical properties was obtained through nano coatings [8].

Materials and Methods

Materials

High-speed tool steel M50 is made of and is a member of the M series of steels. It is renowned for having a superb balance of toughness, wear resistance, and high hot hardness, making it appropriate for use in a variety of cutting tool applications [9]. Milling cutters, reamers, broaches, taps, drills, and other high-performance cutting tools are frequently made from M50 steel [10]. Gas nitriding is a surface hardening method that can be used to improve the wear resistance, fatigue strength, and overall surface hardness of M50 steel and other steel alloys [11]. When M50 steel is subjected to gas nitriding, it is heated to temperatures between 500 °C (932 °F) and 600 °C (1112 °F) while being exposed to a nitrogen-rich environment. The nitrogen atoms infiltrate into the steel's surface layer throughout the process, generating a nitride layer.

When preparing a specimen with EDM cutting, an electrode (tool) is used to create a regulated electrical discharge between the workpiece, which is normally submerged in a dielectric fluid [12]. The substance is melted and vaporized by the discharge's extreme heat, which is subsequently removed by the dielectric fluid. The workpiece is efficiently cut or shaped in accordance with the intended design by repeating this procedure in a succession of quick electrical discharges. The specimen must meet the specifications of 25 mm starting diameter and EDM square-cut samples measuring 10 mm x 10 mm.

The seawater solution procedure addresses obtaining clean and filtered water. The foundation of sea water solution should be clean, distilled, or deionized water. Make sure the water is clear of pollutants and impurities that can affect how accurate the readings are. A 1000 ml glass jar is filled with 800 ml of

distilled water. The chemicals are weighed in accordance with the specifications using an electron weigh balance machine, and then they are added to the initial solution. The previous solution is now diluted with distilled water until it contains 1000 ml. Following the complete dissolution of the added compounds, the solution is used for an experiment.

Methodology

A working electrode, a reference electrode, and a counter electrode should be prepared for a three-electrode system. The appropriate substance for the electrochemical reaction is typically coated on or manufactured into the working electrode. Metals, carbon-based materials, and modified electrodes with particular catalysts are popular options [13].

Select a reference electrode with an electrochemical potential that is stable and well-defined. The standard hydrogen electrode is the reference electrode that is most frequently used, but other references can also be utilized, such as the saturated calomel electrode or the silver/silver chloride electrode, depending on the needs of the experiment. In order to complete the electrical circuit, the counter electrode—typically constructed of platinum or graphite—is required. Connect the potentiostat to the reference electrode and calibrate it by changing the voltage until it matches the reference electrode's known potential before beginning the real measurements. As a result, the experiment's potential measurements are accurate [14].

Place the working, reference, and counter electrodes in an electrolyte cell or solution that is appropriate for the experiment at hand. Using the potentiostat, apply a regulated voltage to the working electrode relative to the reference electrode. The voltage can be continually swept or changed over a particular range. The electrochemical reaction occurring at the electrode surface is directly related to the resultant current that travels through the working electrode. Depending on the experiment, the current can be measured in a variety of ways, including voltammetrically (sweeping the voltage and measuring the resulting current), potentiostatically (maintaining a constant voltage), and amperometrically (measuring a steady-state current). To comprehend the electrochemical behavior of the species under study, analyze the collected current-voltage data. In order to do this, the data must be plotted as a voltammogram, a graph that displays the current as a function of the applied voltage. Extract important electrochemical information from the voltammogram, such as peak currents, oxidation and reduction potentials, and curve shapes. These variables reveal details regarding the species' redox behavior, kinetics, and stability. To determine the reactivity and stability of the electrochemical system, compare the collected data with established reference values or theoretical hypotheses.

Corrosion behavior of heat treated M50 steel

Testing materials like M50 steel for corrosion resistance using electro-potentiodynamic corrosion is a routine practice. This method of testing evaluates the corrosion behavior of the material by applying a regulated voltage and measuring the resulting current. Further study using potentiodynamic methods is also possible. For example, the polarization curve

can be fitted to Tafel equations or impedance data can be extracted using electrochemical impedance spectroscopy, giving more thorough understanding of the corrosion behavior. Prepare test specimens made of M50 steel that are the proper size and shape. Make sure the surfaces are spotless and devoid of any impurities that can affect the test results. The type of electrode(s) to employ in the test arrangement should be decided. A counter electrode and a reference electrode are typical options. The working electrode is a piece of M50 steel. Choose an electrolyte solution that is appropriate for the desired application or testing needs and simulates a corrosive environment. To accurately evaluate the M50 steel's corrosion resistance, the electrolyte needs to replicate the environmental factors that the material would encounter. The electrochemical cell should be set up for testing. The M50 steel specimen, reference electrode, and counter electrode are normally submerged in the electrolyte solution. Ensure solid setup and adequate electrical connections. Measurement of the OCP leave the system at rest for a while to allow it to attain a stable condition. The M50 steel specimen's OCP in the electrolyte should be measured. This potential shows the material's initial corrosion behavior.

Apply a controlled potential while scanning the potential within a predetermined range to the working electrode (M50 steel). Both the cathodic (negative) and anodic (positive) orientations sweep the potential. Through scanning, a polarization curve is produced that contains details regarding the kinetics of corrosion, its potential (E_{corr}), and its current density (I_{corr}). Record the resulting current response at various potentials during the potentiodynamic scan. The data gathered can be used to determine variables like polarization resistance (R_p), corrosion rate, corrosion potential, and passivation potential. These factors aid in assessing M50 steel's behavior and corrosion resistance. To evaluate the corrosion resistance of M50 steel, analyze the collected data and compare it to established standards or reference materials. Aspects including corrosion potential, rate, and the existence of passivation or active corrosion zones should be taken into account.

Results and Discussion

We can observe that the OCP test was conducted in the plot below (Figure 1). A total of 10 samples of M50 material underwent heat treatment, and the OCV corrosion rate test was conducted. We can see in the graph above that the corrosion resistance of the 10 samples has changed across a variety of time periods. The corrosion resistance will break down and fully lose its strength of resistance when the corrosion line is diverted. Therefore, it took more time to obtain the corrosion resistance in graph for sample 6. Table 1 presents E_{corr} values for gas nitrided samples.

Step 1

The corrosion resistance in the anodic region in figure 2 is somewhat reducing its resistance. The breaking point of a line is when it becomes entirely straight. All remaining corrosion resistance has been released. Therefore, the corrosion rate of the M50 at 500 °C for 8 h is 38.345. As a result, other samples with greater corrosion resistance should be used instead of the raw sample.

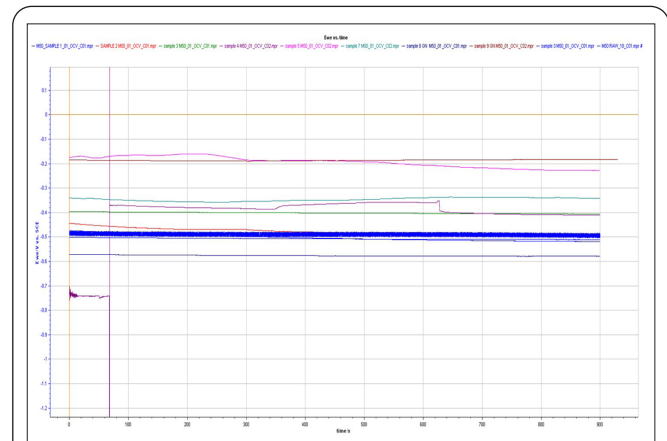


Figure 1: OCP plot for sample 1 to sample 10.

Table 1: E_{corr} values for gas nitrided samples.

Sample number	Sample name	E_{corr} in (mv)	Corrosion rate (mpy)	OCV
1	500-08h	498.772	38.245	-0.5031V
2	500-12h	-576.707	27.6684	-0.4785V
3	500-24h	-679.203	20.1234	-0.4018V
4	520-08h	-524.729	44.2781	-0.4765V
5	520-12h	-302.988	4.25817	-0.1925V
6	520-24h	-654.711	112.123	-0.5074V
7	550-08h	-302.371	25.6767	-0.3461V
8	550-12h	-620.824	64.6518	-0.5764V
9	550-24h	-293.047	2.0207	-0.186V
10	Raw sample	-437.247	9.34665	-0.4896V

Step 2

The corrosion resistance in the anodic region in figure 2 is somewhat reducing its resistance. The breaking point of a line is when it becomes entirely straight. In this figure, the M50 sample is heat treated for 8 h at a corrosion rate of 27.6684 mpy before being gas nitrided at 500 °C for 12 h, which offers superior corrosion resistance.

Step 3

The corrosion resistance at the anodic region in figure 2 is somewhat lowering its resistance. The breaking point of a line is when it becomes entirely straight. The M50 sample in this plot is gas nitrided at 500 °C for 24 h, which further lowers the corrosion rate and improves corrosion resistance compared to the samples that are heat treated at 500 °C for 8 or 12 h, respectively, with corrosion rates of just 20.1234 mpy.

Step 4

As shown in figure 2, the corrosion resistance in the anodic zone is only marginally reducing the resistance. The breaking point of a line is when it becomes entirely straight. The M50 sample in this plot is gas nitrided at 520 °C for 8 h, and it has a corrosion rate that is higher than all other M50 samples tested at 500 °C (44.2781 mpy). Therefore, this sample is likewise unsuitable since it does not provide a very low corrosion rate.

Step 5

The corrosion resistance at the anodic region in figure 2 is

slightly reducing the resistance of it. The breaking point of a line is when it becomes entirely straight. Given that the M50 sample in this plot underwent gas nitriding at 520 °C for 12 h and had the second-lowest corrosion rate of the 10 samples we analyzed, we can conclude that these conditions represent the ideal temperature and time for a sample to undergo heat treatment. With a corrosion rate of 4.258 mpy, this is a good replacement for the raw sample since it offers greater corrosion resistance than any other sample.

Step 6

The corrosion resistance at the anodic region in figure 2 is slightly reducing the resistance of it. The breaking point of a line is when it becomes entirely straight. The M50 sample, which was gas nitrided at 520 °C for 24 h, has the greatest rate of corrosion of any heat-treated sample, measuring 112.123 mpy.

Step 7

As shown in figure 2, the resistance to corrosion in the anodic zone is somewhat lowering. The breaking point of a line is when it becomes entirely straight. Although the M50 sample in this plot has strong corrosion resistance with a corrosion rate of 25.67 mpy and was gas nitrided at 550 °C for 8 h, it is still not ideal because we have alternative samples with superior corrosion resistance qualities.

Step 8

The corrosion resistance at the anodic region in figure 2 is slightly reducing the resistance of it. The breaking point of a line is when it becomes entirely straight. Since the corrosion rate of the M50 sample, which was gas nitrided at 550 °C for 12 h, was much higher than that of the other samples in this plot (65.65 mpy), it was not appropriate to use this sample in place of the raw sample.

Step 9

The corrosion resistance at the anodic area is somewhat lowering the resistance of it in figure 2. The breaking point of a line is when it becomes entirely straight. The M50 sample, which was gas nitrided at 550 °C for 24 h, is the best sample in the group and can take the place of the raw sample since it has the best corrosion resistance of all the 10 samples tested and a very low corrosion rate of 2.027 mpy.

Step 10

The corrosion resistance at the anodic region is somewhat lowering the resistance of it in figure 2. The breaking point of a line is when it becomes entirely straight. With a corrosion rate of 119.34 mpy, the M50 sample in this plot has the greatest corrosion rate of all the samples studied here and is not heat treated. It also has very poor mechanical qualities.

Conclusion

Based on the data and graph above, we can draw the conclusion that heat treatment and temperatures at which solutions are formed have a significant impact on mechanical attributes and corrosion rate values. However, the best temperatures must be chosen in order to provide the best mechan-

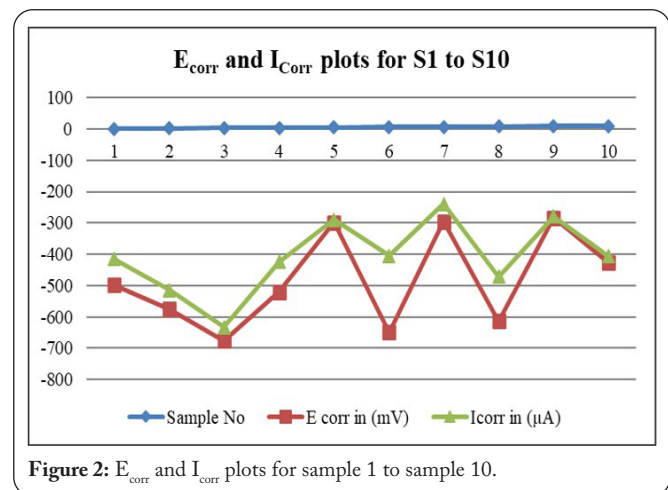


Figure 2: E_{corr} and I_{corr} plots for sample 1 to sample 10.

ical qualities and corrosion resistance properties. The findings of the gas nitrided heat treatment on the bearing steel M50 material demonstrate an OCV incorporating corrosion resistance. We can obtain materials that are gas nitrided coated by doing the heat treatment on various samples at various temperatures. After the corrosion test was completed, the material M50 with a temperature of 520 °C for 12 h had a lower corrosion rate than the other samples. As a result, the 520 °C at 12 h have the lengthy amount of time to resist by employing heat treatment procedure and corrosion test. In this experiment, we found that the optimal temperature is M50 at 520 °C for 12 h, which has better corrosion resistance than any other sample tested. The corrosion resistance also improved on the gas nitrided samples when compared to the raw sample, so we can conclude that heat treating improves the corrosion resistance of the samples and they also improve the mechanical properties of the samples.

Acknowledgements

None.

Conflict of Interest

None.

References

1. Yao J, Yan F, Chen B, Yang Y, Xu Y, et al. 2021. Dual-strengthening of steel surface and bulk via synergistic effect of plasma nitriding: a case study of M50 steel. *Surf Coat Technol* 409: 126910. <https://doi.org/10.1016/j.surfcoat.2021.126910>
2. Yan MF, Wang XA, Liu RL, Zhang YX, Yang Y. 2017. Kinetics and wear behaviour of M50NiL steel plasma nitrided at low temperature. *Mater Sci Technol* 33(3): 370-376. <https://doi.org/10.1080/02670836.2016.1213027>
3. Yao JW, Yan FY, Yan MF, Zhang YX, Huang DM, et al. 2019. The mechanism of surface nanocrystallization during plasma nitriding. *Appl Surf Sci* 488: 462-467. <https://doi.org/10.1016/j.apsusc.2019.05.164>
4. Li Z, Tang G, Ma X, Sun M, Wang L. 2010. XPS study on chemical state and phase structure of PBII nitriding M50 steel. *IEEE Trans Plasma Sci* 38(11): 3079-3082. <https://doi.org/10.1109/TPS.2010.2050075>
5. Lina T, Mufu Y. 2012. Microstructure and mechanical properties of surface layers of 30CrMnSiA steel plasma nitrocarburized with rare earth addition. *J Rare Earths* 30(12): 1281-1286. [https://doi.org/10.1016/S1002-0721\(12\)60221-X](https://doi.org/10.1016/S1002-0721(12)60221-X)

6. Kusmic D, Van Thanh D. 2017. Tribological and corrosion properties of plasma nitrided and nitrocarburized 42CrMo4 steel. *IOP Conf Ser Mater Sci Eng* 179(1): 012046. <https://doi.org/10.1088/1757-899X/179/1/012046>
7. Yu Y, Shironita S, Nakatsuyama K, Souma K, Umeda M. 2016. Influence of nitriding surface treatment on corrosion characteristics of Ni-free SUS445 stainless steel. *Electrochemistry* 84(9): 709-713. <https://doi.org/10.5796/electrochemistry.84.709>
8. Gu Y, Xia K, Wu D, Mou J, Zheng S. 2020. Technical characteristics and wear-resistant mechanism of nano coatings: a review. *Coatings* 10(3): 233. <https://doi.org/10.3390/coatings10030233>
9. Yuan J, Zhu K, Jiang J, Zhang H, Fu A, et al. 2020. Corrosion behavior of Cr-bearing steels in CO₂-O₂-H₂O multi-thermal-fluid environment. *Mater Res Express* 7(10): 106518. <https://doi.org/10.1088/2053-1591/abbfbc>
10. Venkatesh B, Shiva M, Reddy C, Chaitnaya U. 2022. Corrosive behavior of 440C and M50 steels for marine applications. *AIP Conf Proc* 2648(1): 030010. <https://doi.org/10.1063/5.0114398>
11. Kumar R, Alphonsa J, Prakash R, Boob KS, Ghanshyam J, et al. 2011. Plasma nitriding of AISI 52100 ball bearing steel and effect of heat treatment on nitrided layer. *Bull Mater Sci* 34(1): 153-159. <https://doi.org/10.1007/s12034-011-0065-9>
12. Nam ND, Xuan NA, Van Bach N, Nhung LT, Chieu LT. 2019. Control gas nitriding process: a review. *J Mech Eng Res Dev* 42: 17-25.
13. Wang B, Zhou S, Wang J, Zhao B. 2014. Effect of gas nitriding on CO₂ corrosion for 35CrMo steel after surface nanocrystallization. *J Nanosci Nanotechnol* 14(10): 8079-8082. <https://doi.org/10.1166/jnn.2014.9400>
14. Yan F, Chen B, Yao J, Zhang D, Yan MF, et al. 2021. Characterization of microstructure and corrosion properties of AZ91D magnesium alloy surface-treated by coating-nitriding. *J Mater Res Technol* 14: 1559-1568. <https://doi.org/10.1016/j.jmrt.2021.07.065>